Heterogeneous Reactions of Linoleic Acid and Linolenic Acid Particles with Ozone: Reaction Pathways and Changes in Particle Mass, Hygroscopicity, and Morphology

Alex K. Y. Lee and Chak K. Chan*

Department of Chemical Engineering, Hong Kong University of Science and Technology, Clear Water Bay, Kowloon, Hong Kong

In this study, an electrodynamic balance (EDB) and a single particle Raman spectroscopic system were used to investigate the heterogeneous reactions of linoleic acid and linolenic acid with ozone under ambient temperatures (22−24 °C) and dry conditions (RH < 5%). Raman characterizations provide evidence that ozone-induced autoxidation, in addition to direct ozonolysis, is a plausible pathway in the reactions between ozone and linoleic acid and linolenic acid particles. Furthermore, the significance of this specific oxidation pathway depends on the ozone concentrations used in the experiment. A low ozone concentration (∼200−250 ppb) with a longer exposure period (20 h) favors autoxidation but an extremely high ozone concentration (∼10 ppm) favors ozonolysis and forces most unsaturated fatty acids to react with ozone in a relatively short period of time. In the low ozone concentration experiments, the mass of the ozone-processed linoleic acid and linolenic acid particles increased by about 2−3% and 10−13%, respectively. In addition, the mass ratios (particle mass at RH ≈ 85% to particle mass at RH < 5%) of the ozone-processed linoleic acid and linolenic acid particles increased by about 2−3% and 3−4%, respectively. The morphology of the pure and ozone-processed linoleic acid and linolenic acid particles are compared, based on imagining and their light scattering patterns.

1. Introduction

Organic compounds are recognized as ubiquitous components of atmospheric aerosols. They consist of hundreds of individual organic species with a wide range of properties.[1] Because of their abundance and diverse functional characteristics, organic components can have significant impacts on both physical and chemical properties of atmospheric aerosols and consequently the global climate.[2,3] For instance, a number of laboratory studies have demonstrated that the presence of organics can modify the hygroscopicity[4−6] and the cloud condensation nuclei (CCN) activity[7,8] of inorganic particles. However, due to interactions with atmospheric oxidants (e.g., ozone, OH, and NO_3 radicals) and gas phase organic reactants, the chemical compositions as well as the properties of atmospheric organic aerosols keep altering throughout their lifetimes[1,9−11] but our understanding of these heterogeneous processes and their potential effects is rather limited.

Ozonolysis of oleic acid has recently emerged as a model system in understanding the chemistry of the heterogeneous oxidation of organic aerosols and their environmental effects. Significant effort has been expended to examine the kinetic parameters, reaction mechanisms, and gas phase and particle phase products of this model system using various experimental approaches.[12−19] It is generally believed that the reaction products formed via oleic acid ozonolysis are consistent with the predictions of the Criegee mechanism even though the relative importance of each specific pathway is still uncertain.[20] Some recent laboratory studies have provided evidence that the reaction products of oleic acid ozonolysis remaining in the particle phase contained both low molecular weight and oligomeric products,[16,17,21] and they were more hygroscopic[19,22] and CCN active[23] than their parent molecules.

Linoleic acid and linolenic acid are polyunsaturated fatty acids that are putatively from leaf abrasion and perhaps meat cooking activities.[24,25] These polyunsaturated fatty acids are the major components of edible oils.[26] The chemical structures of these acids are very similar to oleic acid except for their degree of unsaturation, as shown in Figure 1. Since these two acids contain more carbon−carbon double (C═C) bonds in their hydrocarbon skeletons than oleic acid, they are expected to be more reactive than oleic acid under ozone exposure. A few previous studies have reported that the reactive uptake coefficient of ozone increases with the degree of unsaturation among these three unsaturated fatty acids.[12,14,15] While ozone molecules can directly attack the C═C bonds of linoleic acid and linolenic acid, it is particularly important to note that ozone can also efficiently initiate another oxidative pathway, the so-called autoxidation pathway, of polyunsaturated fatty acids.[27,28] However, to the best of our knowledge, the autoxidation of polyunsaturated fatty acids has not yet been reported in the atmospheric chemistry literature. The significance of this specific oxidation pathway needs to be investigated.

Recently, our group has demonstrated the combined use of the electrodynamic balance (EDB) and Raman spectroscopy of single levitated particles to study the ozonolysis of oleic acid particles.[19] One of the distinct advantages of using our EDB/ Raman system for studying heterogeneous reactions is that long duration exposure of particles to gas phase reactants at concentrations relevant to atmospheric applications is possible as the particles can be trapped inside the EDB for an extended period of time (days). This special feature is important because most previous studies in the literature used gas reactant concentrations that were much higher than atmospheric concentrations to compensate for the short duration of the exposure. Furthermore, our EDB/Raman system also allows *in situ* chemical composition (functional group) analysis of the levitated

* Corresponding author. Telephone: (852) 2358-7124. Fax: (852) 2358-0054. E-mail: keckchan@ust.hk.
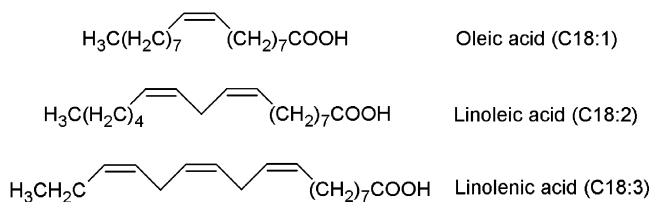
Figure 1. Chemical structures of oleic acid, linoleic acid, and linolenic acid.

particles and direct measurements of particle mass changes due to reactions and the hygroscopicity of the reacted particles. The morphology and laser-illuminated light scattering pattern of the levitated particles can also be monitored and captured using a microscope coupled with a digital camera. In this paper, we present the possible reaction pathways involved when the linoleic acid and linolenic acid particles are exposed to 200−250 ppb of ozone using the EDB/Raman technique. An extremely high ozone concentration (∼10 ppm) was used for comparisons with the results obtained from our low ozone concentration experiments. The changes in particle mass and hygroscopicity caused by the low ozone exposure are also reported. Furthermore, the modifications to particle morphology due to low and high ozone exposure are compared. Our findings potentially lead to a better understanding of the heterogeneous oxidation of organic aerosols and their potential effects in the atmosphere.

2. Experimental Methods

2.1. Generation of Organic Particles. Linoleic acid (>99%, Sigma-Aldrich) was first dissolved in ethanol (>99.9%, Merck). A small amount of this solution was introduced into a piezoelectric particle generator (Uni-Photon Inc., New York, model 201). By applying electric pulses to the droplet generator, solution droplets (∼40−70 μm) were generated and charged by passing through the metal induction plate before they entered into the electrodynamic balance (EDB). An organic droplet was levitated and held stationary with proper adjustments of the combination of ac and dc electric fields inside the EDB. The evaporation of the solvent resulted in pure linoleic acid particles that were used in the reaction studies. Similar procedures were used to prepare linolenic acid (>99%, Sigma-Aldrich) particles.

2.2. Ozone Generation. Ozone was generated from purified dry air (relative humidity (RH) <5%) flowing through a UV light source (Jelight model 600). The ozone concentration was monitored using a portable ozone analyzer (Aeroqual, Series 300 ozone monitor with a low concentration sensor head). The ozone concentration used was in the range of 200−250 ppb. The ozone exposure time for each organic particle was about 20 h under ambient temperatures (22−24 °C) and dry conditions (RH < 5%). This ozone exposure is relevant to atmospheric conditions, assuming that the ambient ozone concentration is about 20−40 ppb and 100−400 ppb in rural and urban environments, respectively.[1] Ozone-containing air was fed to the EDB, which served as a reaction chamber, at a flow rate of approximately 230−250 mL/min. An extremely high ozone concentration (∼10 ppm) was also applied for comparisons with the results obtained in the low ozone concentration experiments. The exposure time for the high ozone concentration was about 2 h.

2.3. The Electrodynamic Balance and Hygroscopic Measurements. The principle of the EDB has been well documented[29] and therefore is not described in detail here. In brief, a charged particle or droplet with about a 40−70 μm diameter

is trapped at the null point of the cell through a combination of dc and ac electric fields surrounding the particle. Assuming that there is no loss of charge, the mass of the particle is proportional to the applied dc voltage. Hence, the relative mass change of the particle due to any physical (e.g., evaporation or condensation of water in response to the changes in ambient RH) or chemical changes was determined by recording the dc voltage required to balance the weight of the particle.

In this study, hygroscopic measurements were made before and after the heterogeneous reactions to investigate the effects of these reactions on the hygroscopicity of the organic aerosols. The experimental results are presented in the form of mass ratios (m/m_0) instead of the mass fraction of solute (mfs) as usually used in hygroscopic measurements in an EDB (e.g., Chan et al.[30]) because the composition of the reacted particles was highly uncertain and thus no bulk data could be used for identification of the reference state.[31] The m/m_0 is the ratio of the particle mass, m, at a given RH to the particle mass, m_0, at the reference RH (RH<5%) at equilibrium. The RH inside the EDB was adjusted by mixing a stream of saturated air and another of dry air at controlled flow rates. The overall experimental error of the mass ratios obtained from the hygroscopic measurements was within 1% for droplets, and the error in the determination of RH was estimated to be ± 1% at RH = 40−80%. In addition to the hygroscopic measurements, the mass changes of the levitated particles caused by chemical reactions were also monitored at 2 h intervals over a total of 20 h of ozone exposure. These measurements were made at RH < 5%.

2.4. Raman Spectroscopy of Single Levitated Particles. We measured the Raman scattering of levitated particles undergoing heterogeneous reactions for aerosol composition (functional group) analyses. In this study, we used a Raman spectroscopy system similar to that used in Zhang and Chan.[32] It consisted of a 5 W argon ion laser (Coherent I90−5) and a 0.5 m monochromator (Acton SpectraPro 500) attached to a CCD (Andor Technology DV420-OE), which was integrated with the EDB system. The 514.5 nm line of an argon ion laser with output power between 25−50 mW was used as the source of excitation. A pair of lenses, which matched the f/7 optics of the monochromator, was used to focus the 90° scattering of the levitated droplet in the EDB onto the slit of the monochromator. A 514.5 nm Raman notch filter was placed between the two lenses to remove the strong Rayleigh scattering. A 300 g/mm grating of the monochromator was selected. The Raman spectra of the stationary organic particles were recorded at 2 h intervals over a total of 20 h of ozone exposure. The integration time of each spectrum was 30 s (10 frames, each with an accumulation time of 3 s). The resolution of the spectra obtained was about 6 cm^{-1}. All measurements were made at ambient temperatures of 22−24 °C.

2.5. Morphology and Light Scattering Pattern Measurements. The morphology and laser-illuminated light scattering pattern of the levitated particles were monitored and captured through the window of the EDB using a microscope (5× objective and 20× eyepiece) coupled with a digital camera (Nikon Cooplix 990). For capturing the images of the particles, the light source was placed at the opposite side of the microscope so that the particle shape could be projected onto the digital camera via the microscope. This approach was used for recording the changes in the particle shapes due to the heterogeneous reactions. In addition, the phase of each particle was determined by analyzing the laser-illuminated light scattering pattern from the levitated particle.[33,34] In this study, a He−Ne laser with a wavelength of 632.8 nm was used as the

Heterogeneous Reactions of Linoleic Acid

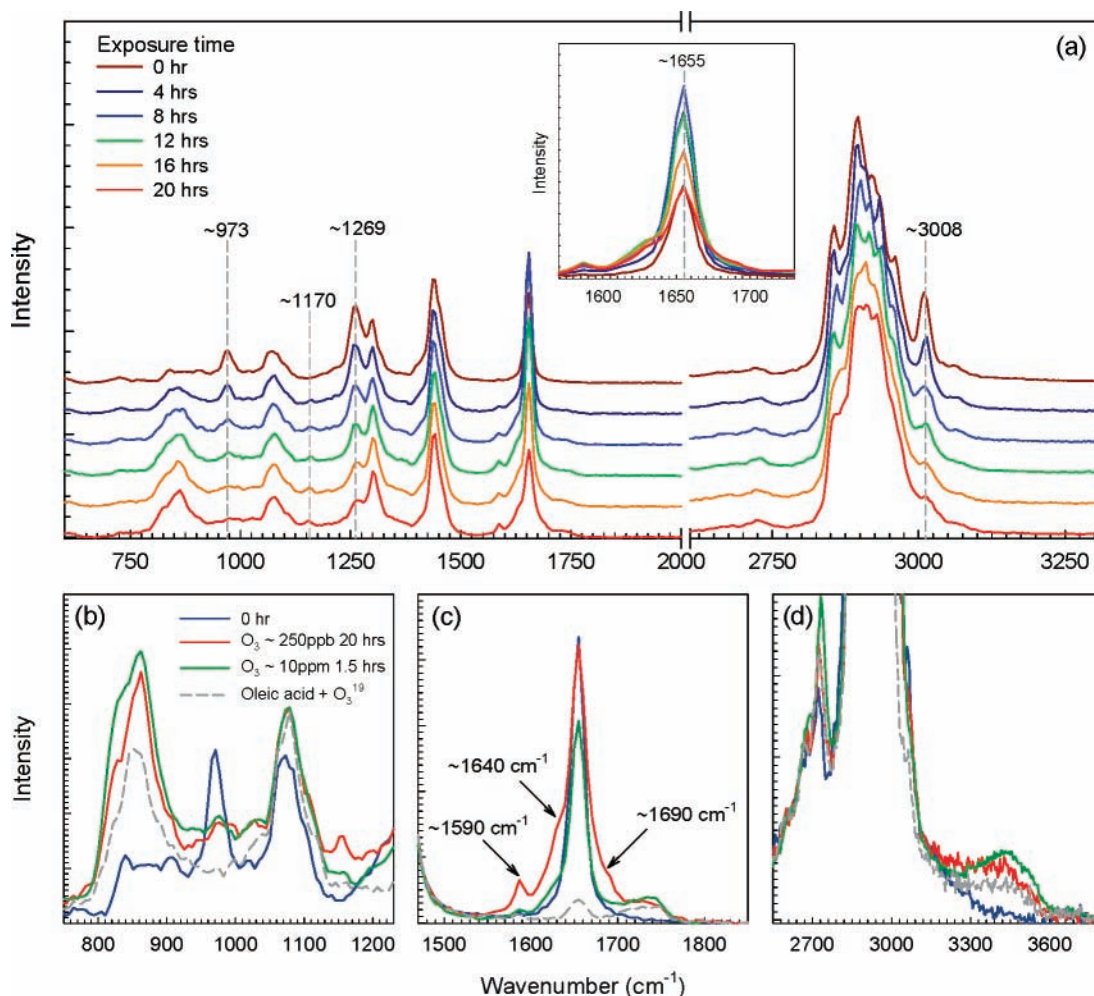*J. Phys. Chem. A, Vol. 111, No. 28, 2007* **6287**

Figure 2. (a) Raman spectra of linoleic acid particles at different ozone exposure obtained in low ozone concentration experiments. Spectral features of ozone-processed linoleic acid particle: Formation of (b) peroxides and ozonides, (c) carbonyl compounds, and (d) hydroxyl compounds obtained in low ($\sim$200$-$250 ppb for 20 h) and high ozone concentration experiments ($\sim$10 ppm for 1.5 h). The Raman spectra are normalized to the peak located at 1443 cm^{-1}. The Raman features of ozone-processed oleic acid particles ($\sim$240$-$280 ppb for 20 h) are shown for comparison.[19]

illuminating source. The laser beam passed through the levitated particle from the bottom of the EDB and the microscope was positioned at an angle of 90° with respect to the laser beam. The light scattering image was first focused so that two clear light spots could be observed via the eyepiece of microscope. After that, the eyepiece was removed to obtain the laser-illuminated light scattering pattern (the particle image was actually out of focus). If the levitated particle was a homogeneous droplet, then the light scattering pattern included some sharp horizontal lines and the number of horizontal lines depended on the particle size. If the levitated particle contained solids or crystalline materials or had an irregular coating, then the light scattering pattern became irregular and fluctuated. Parsons et al.[34] and Olsen et al.[35] used the similar experimental approach to study the nucleation of levitated droplets.

3. Results and Discussion

In this section, we first present the Raman spectra of the levitated linoleic acid and linolenic acid particles obtained in low and high ozone concentration experiments. On the basis of the spectral features of the ozone-processed particles, the possible reaction pathways of the heterogeneous process are outlined and discussed. The modifications to the particle mass and hygroscopicity due to low ozone exposure are also reported. Last, the changes in particle morphology and laser-illuminated light scattering pattern due to low and high ozone exposure are

presented and compared. In total, two or three particles of each acid were studied and representative spectra are shown for discussion.

3.1. Raman Spectra of Ozone-Processed Linoleic Acid and Linolenic Acid Particles. The Raman spectra of ozone-processed linoleic acid and linolenic acid particles at low ozone concentration experiments at different exposure times are shown in Figures 2a and 3a, respectively. Raman measurements were taken at 2 h intervals but only spectra at 4 h intervals are shown here for clarity. The intensities of the characteristic bands of the C=C bonds (973, 1269, and 3008 cm^{-1}) of linoleic acid and linolenic acid decreased with increasing ozone exposure time, suggesting the continuous consumption of C=C bonds when the reactions take place. However, the intensity of the peak at $\sim$1655 cm^{-1} (*cis*-C=C bond stretching) first increased and then decreased during the exposure period as shown in the insets of Figures 2a and 3a. The overall changes in the peak intensity are complicated by the product peaks overlapping at or close to this characteristic peak of the *cis*-C=C bond.

Our previous single particle Raman study reported that oleic acid ozonolysis can consume the C=C bonds of oleic acid and generate peroxidic products (O$-$O, peak at $\sim$850 cm^{-1}), carbonyl (C=O, peak at $\sim$1740 cm^{-1}) and hydroxyl (O$-$H, peak at $\sim$3450 cm^{-1}) groups as shown in Figure 2b$-$d (and more details in Figure S1 of the Supporting Information).[19] In brief, the primary reaction of oleic acid ozonolysis proceeds
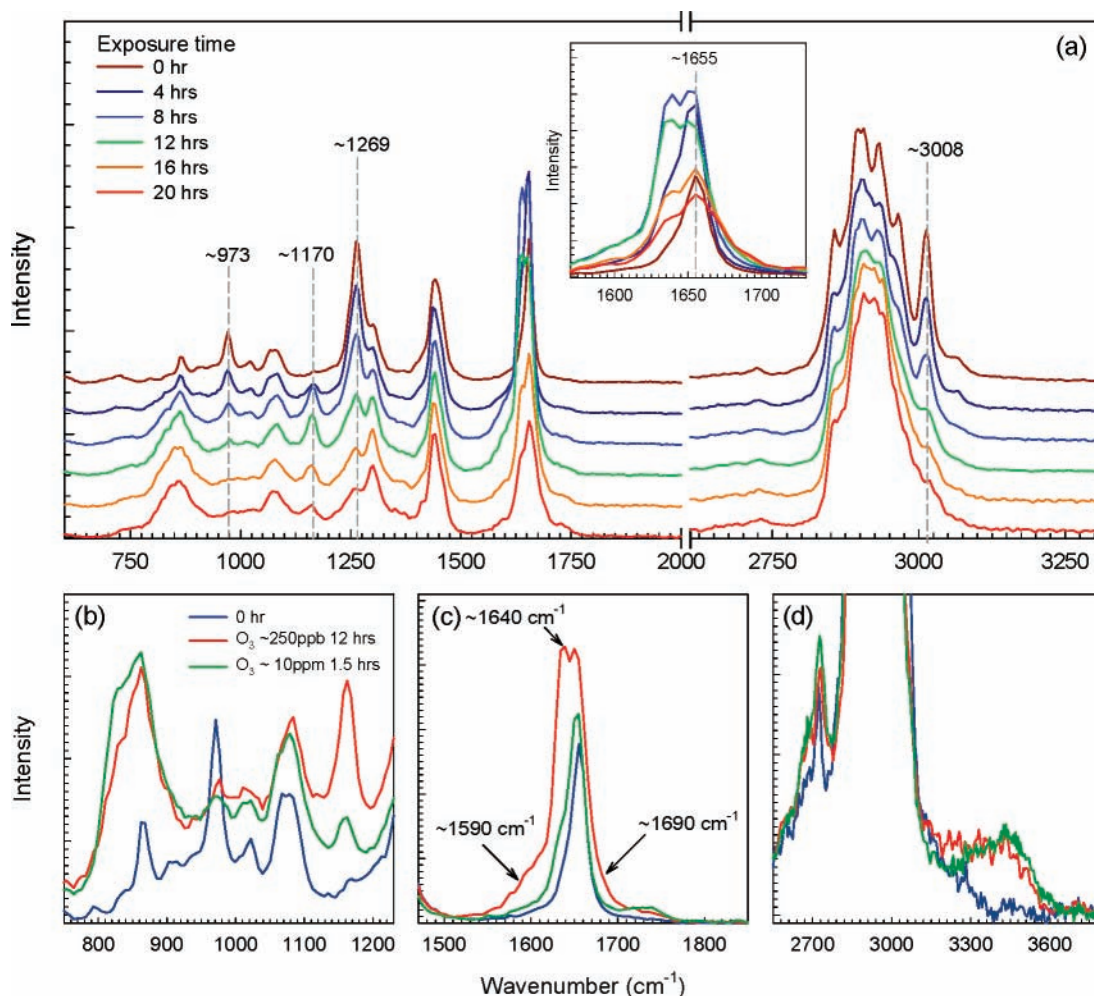
Figure 3. (a) Raman spectra of linolenic acid particles at different ozone exposure obtained in low ozone concentration experiments. Spectral features of ozone-processed linolenic acid particle: Formation of (b) peroxides and ozonides, (c) carbonyl compounds, and (c) hydroxyl compounds obtained in both low (~200−250 ppb for 12 h) and high ozone concentration experiments (~10 ppm for 1.5 h). The Raman spectra are normalized to the peak located at 1443 cm^{-1}.

via the addition of an ozone molecule across the double bond of an oleic acid molecule to form a primary ozonide. The primary ozonide is unstable and thus decomposes to generate carbonyl compounds and Criegee intermediates. Peroxidic products, which are expected to contribute to the Raman signals between 800 and 900 cm^{-1}, are subsequently formed via the reactions between stabilized Criegee intermediates and other existing organic compounds as proposed in the literature.[16,18,20,36,37] Some possible reaction pathways involving stabilized Criegee intermediates are shown in Figure S2 of the Supporting Information. In the low ozone concentration experiments, we also observed similar product peak formation (O−O, C=O, and O−H groups) in the cases of both linoleic acid and linolenic acid as shown in Figures 2b−d and 3b−d, respectively. The close similarities of the functional characteristics of the reaction products generated in the ozone-processed oleic acid, linoleic acid and linolenic acid particles indicate that both linoleic acid and linolenic acid can also undergo direct ozonolysis within the exposure period.

As mentioned previously, there are some product peaks overlapping at or close to the peak at ~1655 cm^{-1} in the low ozone concentration experiments. In general, the C=C stretching vibrations of the conjugated systems (C=C conjugated with C=C or C=O) can generate strong-to-medium Raman signals between the region of 1580−1660 cm^{-1}.[38,39] As shown in Figures 2c and 3c, the strong product peak at ~1640 cm^{-1} is

assigned to the symmetric C=C stretching vibrations of the conjugated dienes (C=C−C=C). The formation of a weak product peak at ~1590 cm^{-1}, which corresponds to the asymmetric C=C stretching vibrations of conjugated dienes, is additional evidence of the appearance of conjugated dienes in the ozone-processed linoleic acid and linolenic acid particles. On the other hand, the product peaks appearing between 1680−1780 cm^{-1} are primarily due to the C=O stretching vibrations of various carbonyl compounds inside the reacted particles. In particular, the Raman signal at ~1690 cm^{-1} is likely caused by the C=O stretching vibrations of C=C−C=O conjugated systems and the conjugations generally enhanced the Raman intensity of the C=O bonds.[26,38]

The Raman spectra of linoleic acid and linolenic acid particles after high ozone concentration exposure (~10 ppm) were also measured as displayed in Figures 2b−d and 3b−d, respectively. The conversion of each acid was similar between the low and high ozone concentration experiments using the normalized peak intensity of the C=C bond at ~1269 cm^{-1} as estimates (data not shown). Hence, direct spectral comparisons are possible to determine whether there was any difference in the reaction pathways between the low and high ozone concentration experiments. The Raman spectra show that a high ozone concentration exposure leads to the formation of O−O, C=O, and O−H functional groups but much less formation of conjugated diene structures (C=C−C=C characteristic peaks
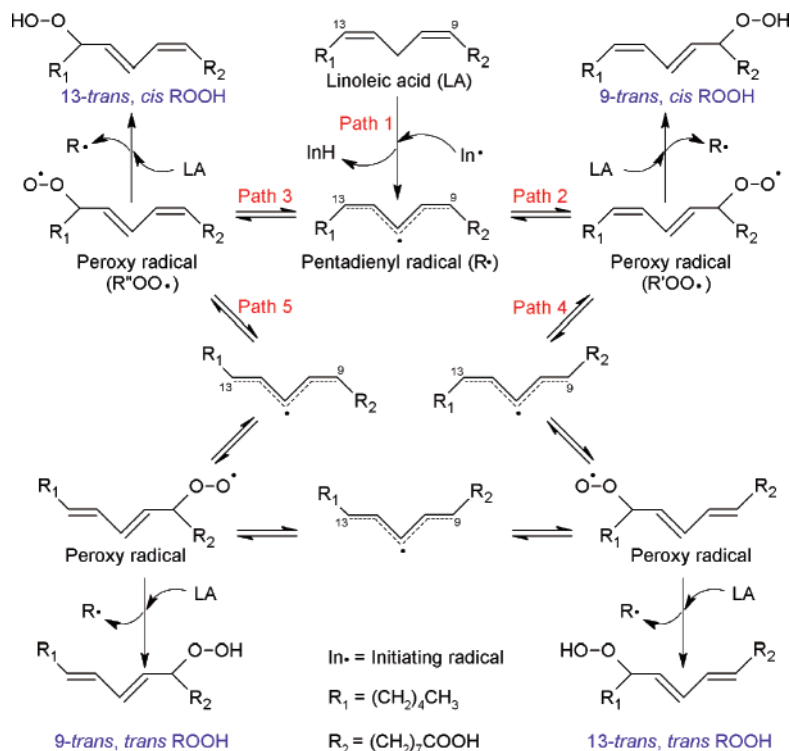
Heterogeneous Reactions of Linoleic Acid

J. Phys. Chem. A, Vol. 111, No. 28, 2007 **6289**

Figure 4. Formation of conjugated diene hydroperoxides via autoxidation of linoleic acid.

at ~1590 and ~1640 cm^{-1} in Figures 2c and 3c). These spectral differences are most obvious in the case of linolenic acid. These observations indicate that there are possibly different dominant reaction pathways between the low and high ozone concentration experiments.

3.2. Autoxidation of Linoleic Acid and Linolenic Acid Particles. There is no doubt that the C=C bonds of linoleic acid and linolenic acid can be directly attacked by ozone molecules, which are similar to the case of oleic acid (Figure S1 and S2) as reflected in the Raman characterizations (O–O, C=O, and O–H groups formation). However, the Raman signatures of the ozone-processed linoleic acid and linolenic acid particles indicate the formation of conjugated dienes (C=C–C=C characteristic peaks at ~1590 and ~1640 cm^{-1}), which cannot be produced via the direct ozonolysis of linoleic acid and linolenic acid, based on the framework of the Criegee mechanism as described in the literature of oleic acid ozonolysis (Figure S2). Instead, they are possibly related to the autoxidation (or peroxidation) of polyunsaturated fatty acids or esters via typical free radical reactions consisting of chain initiation, propagation, and termination steps.[40,41]

The mechanism of methyl linoleate autoxidation has been extensively studied and reviewed in the lipid and food chemistry literature (e.g., Porter et al.;[41] Niki et al.[42]). On the basis of this mechanism, the mechanism of the autoxidation of linoleic acid for the production of four conjugated diene hydroperoxides as the major products is outlined in Figure 4. The initiation step of linoleic acid autoxidation involves the abstraction of a hydrogen atom from the bisallylic carbon (C11) by a chain-initiating radical to produce a pentadienyl radical (R•) (path 1). The propagation step normally begins with the addition of an oxygen molecule to C9 or C13 of the pentadienyl radical to generate *trans*, *cis* peroxy radicals (ROO•), R′OO• in path 2 and R″OO• in path 3. These two peroxy radicals can abstract a hydrogen atom from a donor, such as another linoleic acid, to produce 9- and 13-*trans*,*cis*-conjugated diene hydroperoxides (ROOH). Meanwhile, some pentadienyl radicals (R•) are gener-

ated to activate the normal propagation sequence (R• + O$_2$ → ROO• and ROO• + LA → ROOH + R• in Figure 4). Alternatively, these peroxy radicals may either undergo β-fragmentation to give the original form of pentadienyl radicals (reverse of paths 2 and 3) or new pentadienyl radicals if the bond rotation around C9–C10 of R′OO• (path 4) and C12–13 of R″OO• (path 5) precedes the β-fragmentation. Addition of oxygen to the new pentadienyl radicals ultimately leads to the formation of 9- and 13-*trans*,*trans*-conjugated diene hydroperoxides.

The formation of hydroperoxides from linolenic acid may be understood by using linoleic acid as a model compound. Linolenic acid contains two separate 1,4-diene systems, a C9–C13 system identical to that in the linoleic acid plus a C12–C16 system. As a result, two different pentadienyl radicals can be produced by autoxidation and they can combine with oxygen molecules to generate a complex mixture of 9-, 12-, 13-, and 16-hydroperoxides with conjugated diene structures and various forms of C=C bond geometries.[43,44] However, it is interesting to note that the 12- and 13-hydroperoxides are produced in significantly lower concentrations than the 9- and 16-hydroperoxides as reported in the literature.[43,44] This uneven distribution of hydroperoxides is due to the tendency of 12- and 13-peroxyl radicals to undergo rapid 1,3-cyclization, by intramolecular radical addition to the double bond, to produce cyclic peroxides.[45] The reaction pathways involving the hydrogen abstraction from C14 of the C12–C16 diene structure is outlined in Figure 5 to illustrate the formation of 12- and 16-hydroperoxides and cyclic peroxide products. Peroxy radical cyclization is an important process only in the autoxidation of fatty acids or esters with more than two double bonds, such as linolenic acid and arachidonic acid.[41]

The autoxidation of polyunsaturated fatty acids or esters starts with an induction period, during which the formation of hydroperoxides and conjugated dienes is slow or not yet started, before the rapid and steady formation of reaction products. The induction period of autoxidation varies among species and can
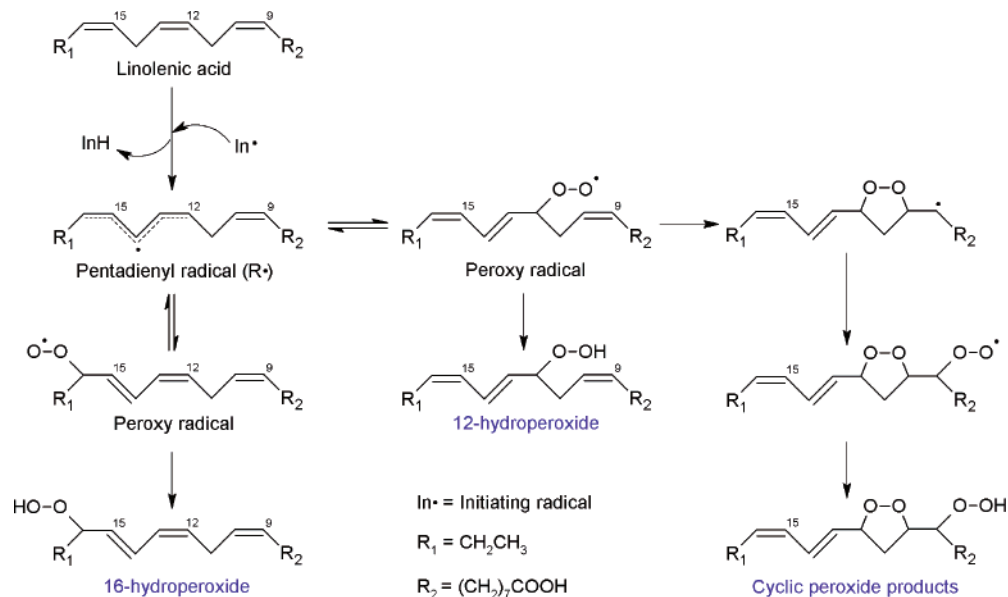
Figure 5. Formation of conjugated diene hydroperoxides and cyclic peroxide products via autoxidation of linolenic acid.
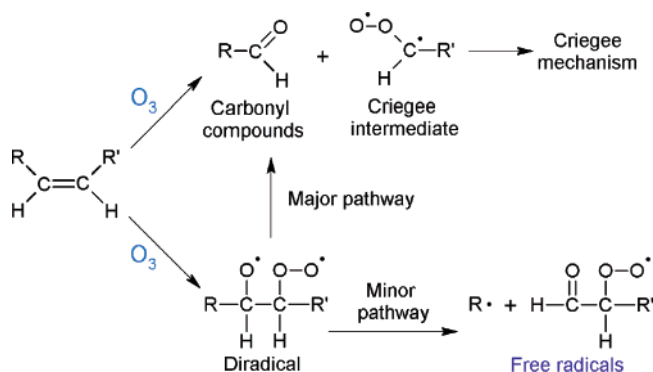

Figure 6. Initiation step of ozone-induced autoxidation.

be markedly reduced by some external factors, such as thermal stress. Atmospheric oxidants such as ozone can also play an important role to speed up this oxidative process.[28] Pryor et al.[27] studied the effect of ozone on the autoxidation of methyl linoleate and methyl linolenate by monitoring the product yields of hydroperoxides and conjugated dienes. They reported that induction periods of the autoxidation of methyl linoleate and methyl linolenate were about 120 and 60 h, respectively, under ozone-free conditions, but were not observed (≈0 h) at ozone concentrations of 350 ppb or above. Their measurements showed that autoxidation of polyunsaturated methyl esters can be initiated effectively with appropriate ozone exposure.

A key event in the initiation of this oxidative process is the formation of radicals as initiators. It is important to note that ozone is not a free radical and therefore cannot initiate autoxidation by itself. There should be at least one pathway that generates free radicals to achieve the initiation step. Pryor[28] argued that reactions of ozone and alkene, such as ozonolysis of unsaturated fatty acids in our study, could be important routes for free radical production. In general, the major decomposition pathway of an energy-rich primary ozonide (or 1,2,3-trioxolane) is the production of the Criegee intermediates and carbonyl compounds in one step. Alternatively, Pryor[28] proposed that trioxolane may homolyze to form a diradical as shown in Figure 6. This diradical can either split in the usual way to produce the Criegee intermediate and a carbonyl compound, or undergo β-scission to split off an alkyl radical (R•) from the alkyl group

that had been attached to the C=C bonds. Pryor et al.[27] observed that once the autoxidation is initiated, the radicals (such as R• shown in Figure 6) produced by ozonolysis of alkene would be negligible relative to the radicals produced by the propagation step of the autoxidation process as shown in Figure 4. However, it must be emphasized that the β-scission step is expected to be only a minor decomposition pathway.

On the basis of the observations by Pryor et al.[27] and our Raman characterizations, it is reasonable to suggest that the autoxidation of linoleic acid and linolenic acid can also be initiated within a short period of time under the ozone concentrations (~200−250 ppb) used in the current study. The induction periods of these two fatty acids are probably reduced to less than 2 h (or even shorter as the time resolution is not high enough to trace the exact induction periods) if we use the change in the intensity of the product peaks of the conjugated dienes at 1560−1640 cm^{-1} as the estimations (Figure 7). In addition to the formation of product peaks at ~1590 and ~1640 cm^{-1}, a new band that peaks at ~1170 cm^{-1} (Figures 2a−b and 3a−b) is additional evidence of the autoxidation mechanisms as this peak has been observed in reported studies of lipid or oil autoxidation (e.g., Tachikawa et al.;[46] Muik et al.[26]). This peak, as well as the peaks at ~1590 and ~1640 cm^{-1}, is appreciably more intense for linolenic acid particles, which is consistent with the fact that linolenic acid is more likely to undergo autoxidation. Gunstone[43] reported the relative rates of autoxidation of oleic acid to linoleic acid to linolenic acid to be 1:27:77.

Overall, the information in the literature and our observed Raman spectra give us confidence that ozone-induced autoxidation, in addition to direct ozonolysis, is a plausible pathway in the reactions between ozone and linoleic acid and linolenic acid particles. Last, it is important to point out that low ozone levels (~200−250 ppb) favor the autoxidation pathways compared with high ozone levels (~10 ppm) as indicated by our Raman measurements (Figures 2c and 3c). Figures 2b and 3b also show that the intensity of the peak at ~1170 cm^{-1} is more intense in the low ozone concentration experiments. A possible explanation for this is that most polyunsaturated fatty acids are forced to react rapidly with ozone molecules under extremely high ozone concentrations instead of undergoing autoxidation.
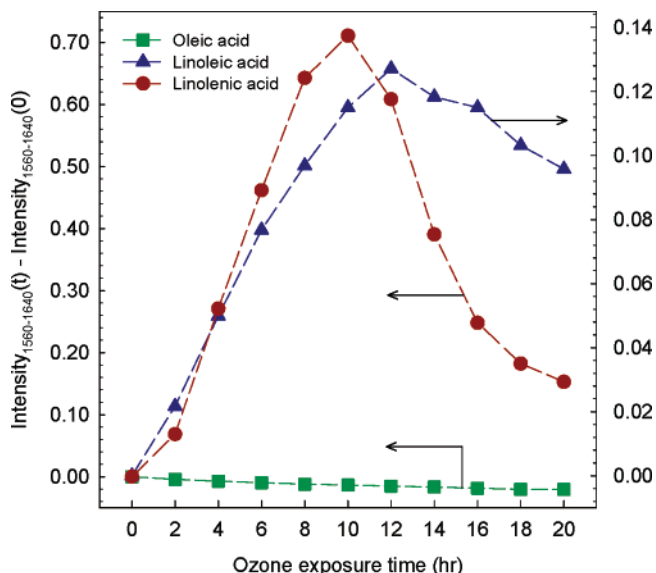
Heterogeneous Reactions of Linoleic Acid

J. Phys. Chem. A, Vol. 111, No. 28, 2007 **6291**

Figure 7. Changes in the peak intensity from 1560 cm^{-1} to 1640 cm^{-1} (C=C−C=C structures) of the polyunsaturated fatty acid particles (green squares: oleic acid, blue triangles: linoleic acid, red circles: linolenic acid) after different ozone exposure periods. The Raman intensities of these peaks are normalized to the intensity of the peak located at 1443 cm^{-1}. The experimental errors are within 10%.

3.3. Ozonolysis of the Autoxidation Products. As discussed in the previous section, autoxidation of linoleic acid and linolenic acid likely took place in the particles with the low ozone concentrations in this study. Since autoxidation would not eliminate the number of C=C bonds in the hydrocarbon skeletons of fatty acid molecules (Figure 4 and 5), ozone can also react with the autoxidation products by attacking their C=C bonds. The ozonolysis of the autoxidation products can be evaluated by monitoring the intensity changes of the distinct Raman signals of conjugated dienes ranging from 1560 to 1640 cm^{-1} (Figure 7). In the case of linolenic acid, the intensity of these two peaks increased rapidly and started to decline after 10−12 h of ozone exposure (left axis of Figure 7). The two-step kinetic behavior indicates the complex chemical mechanism involving accumulation of the intermediate products followed by their loss. The initial rapid increase in Raman intensities suggests that ozone-induced autoxidation is the prevailing reaction pathway, and it is much faster than the decomposition of the conjugated diene hydroperoxides via ozonolysis. During the latter period of exposure, the rate of autoxidation slows down due to depletion of linolenic acid and the ozonolysis of the autoxidation products becomes more dominant, leading to a decrease in the Raman signals. This analysis can be also applied to the case of linoleic acid (right axis of Figure 7) even though the Raman intensity in this range increased slowly, without a significant decrease during the latter period of exposure. In contrast, no Raman signal corresponding to the conjugated diene structures was observed in the ozone-processed oleic acid particle as shown in Figures 2c and 7.[19] This is consistent with the fact that conjugated diene would not be produced even if autoxidation of oleic acid take place inside the particles.[40]

The ozonolysis of the conjugated diene can generate products consisting of C=C−C=O conjugated systems in their hydrocarbon skeletons based on the predictions of the Criegee mechanism. For example, Figure 8 shows the formation of C=C−C=O conjugated structures via ozonolysis of 9-*trans,cis*-conjugated diene hydroperoxide, which can be produced by the autoxidation of linoleic acid (Figure 4). The continuous increase in the peak intensity ranging from 1686 to 1697 cm^{-1}, as shown
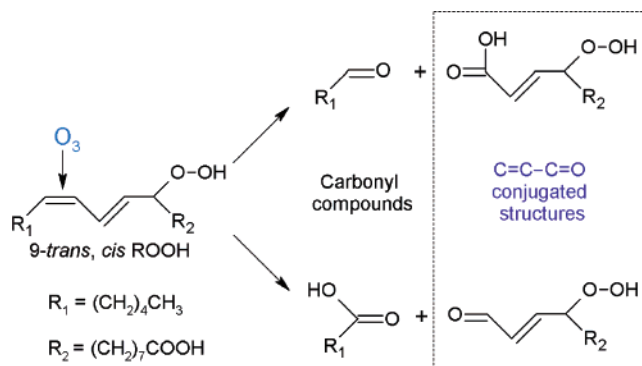

Figure 8. Formation of C=C−C=O conjugated structures via ozonolysis of conjugated diene hydroperoxides.

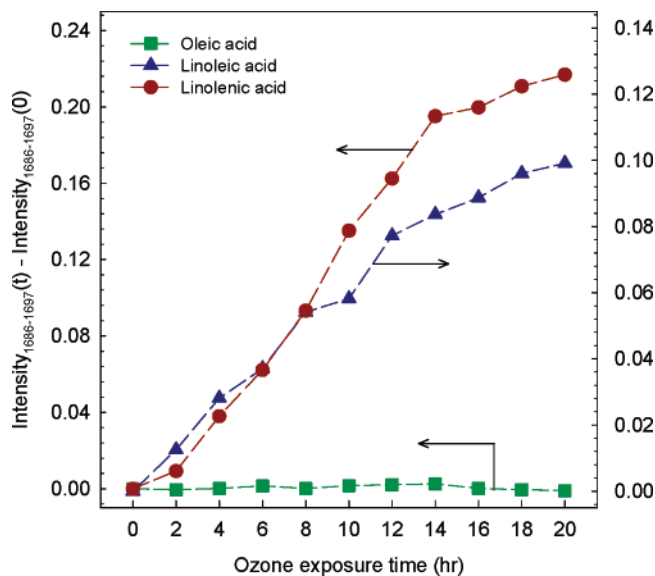**Figure 9.** Changes in the peak intensity from 1686 cm^{-1} to 1697 cm^{-1} (C=C−C=O structures) of the polyunsaturated fatty acid particles (green squares, oleic acid; blue triangles, linoleic acid; red circles, linolenic acid) after different ozone exposure periods. The Raman intensities of these peaks are normalized to the intensity of the peak located at 1443 cm^{-1}. The experimental errors are within 10%

in Figure 9, for both linoleic acid and linolenic acid particles is an indication of the ozonolysis of the intermediate products produced by ozone-induced autoxidation (see also the insets of Figures 2a and 3a). The result of oleic acid ozonolysis is also presented in Figure 9, which indicates that there was no formation of the C=C−C=O conjugated system.[19] As mentioned previously, linolenic acid is more favorable to undergo autoxidation than linoleic acid, and therefore the ozone-processed linolenic acid particles had a larger production of C=C−C=O conjugated structures than the ozone-processed linoleic acid particles. However, Moise and Rudich[12] proposed that 3-nonenal produced via linoleic acid ozonolysis may transform to 2-nonenal. The migration of the C=C bonds from position 3 to position 2 may possibly increase the stability of this aldehyde by forming the C=C−C=O conjugated system. By analogy, this kind of chemical structure transformation may also occur in other possible reaction products such as 12-oxo-9-dodecenoic acid (migration from position 9 to position 10).

3.4. Changes in Particle Mass. The relative mass changes of the ozone-processed linoleic acid and linolenic acid particles in low ozone concentration experiments were determined for different ozone exposure durations. Since the measurements were conducted under dry conditions (RH < 5%) to eliminate
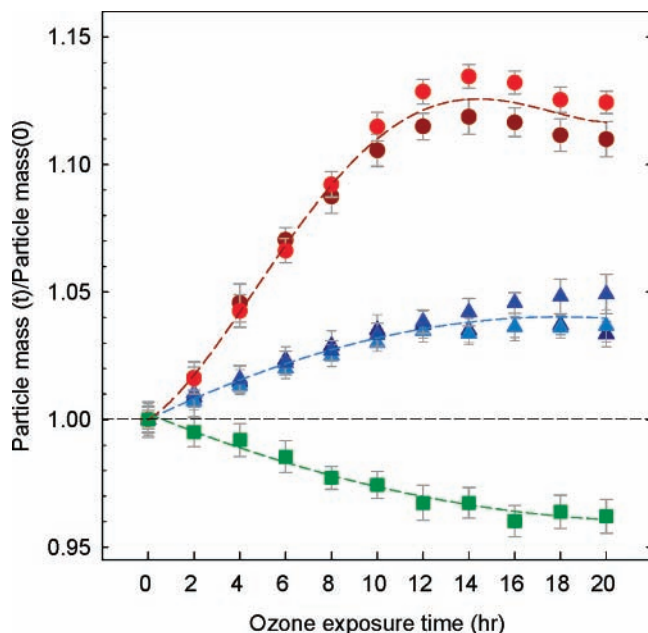
Figure 10. Particle mass changes of oleic acid (green squares, one particle),[19] linoleic acid (blue triangles, three particles) and linolenic acid (red circles, two particles) particles during ozone exposure periods. The lines are to guide the eye and have no physical meaning.

Figure 11. Hygroscopicity of the pure polyunsaturated fatty acids (open triangles, linoleic acid, two particles; open circles, linolenic acid, one particle) and ozone-processed linoleic acid (solid blue triangles, three particles) and linolenic acid (solid red circles, two particles) particles. The lines are to guide the eye and have no physical meaning.

water uptake, the relative mass changes of the particles were caused by the evaporation loss of volatile organic products as well as the mass gain caused by the addition of oxygen and ozone molecules via autoxidation and ozonolysis, respectively. Figure 10 shows the mass ratios (particle mass at time *t* to the initial particle mass) of the ozone-processed unsaturated fatty acid particles as a function of the ozone exposure time. The mass of the ozone-processed linoleic acid and linolenic acid particles increased by about 2−3% and 10−13%, respectively, compared with their original masses. The mass changes of ozone-processed oleic acid particles as a function of exposure time are also shown in Figure 10 for comparison.[19] The mass of oleic acid particles decreased by about 3−4% after 20 h of ozone exposure. It is worth noting that the mass of the ozone-processed linoleic acid and linolenic acid particles initially increased rapidly and then slightly declined or remained at constant level. This two-step behavior indicates that less volatile organic species were the predominant products at the beginning followed by generation of more volatile species in the later exposure period.

Our direct mass measurements show that heterogeneous oxidation of organic aerosols can either increase or decrease the particle mass yields to different extents depending on the molecular structures of the chemical species. There are two possible reasons for the mass gain of ozone-processed linoleic acid and linolenic acid particles. First, autoxidation is expected to be the predominant reaction pathway at the beginning. According to Figures 4 and 5, autoxidation pathways did not break down the skeleton of these two fatty acids to generate volatile species. Instead, the autoxidation pathways involve the addition of oxygen molecules to increase the molecular weight of the fatty acids (paths 2 and 3 in Figure 4). The mass gain in the linolenic acid particles is the most significant because linolenic acid is the species that most favors autoxidation among the fatty acids studied here. It should be noted that oleic acid cannot undergo autoxidation except under elevated temperature conditions because the bond dissociation energy of an allylic hydrogen (e.g., hydrogen atom at C8 and C11 of oleic acid) is
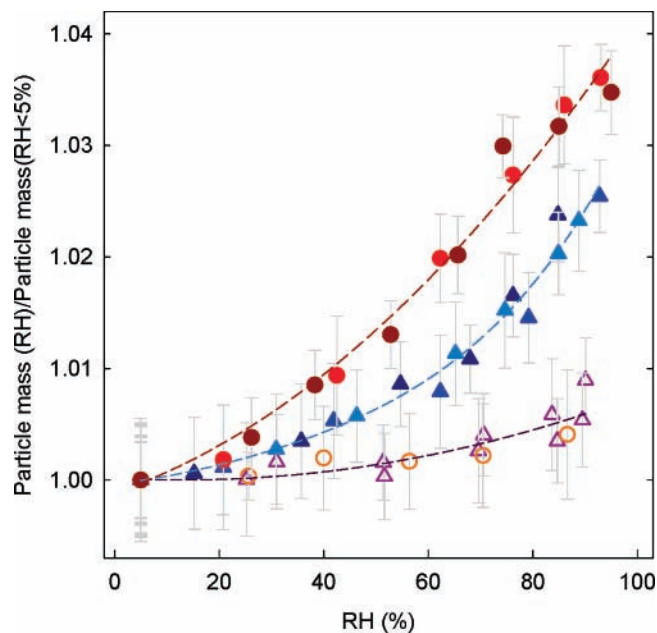
approximately 10 kcal/mol greater than that of bisallylic hydrogen (e.g., hydrogen atom at C11 of linoleic acid).[41] Therefore, the mass loss in the ozone-processed oleic acid particles was mainly caused by the evaporative loss of volatile organic products (e.g., nonanal) formed via ozonolysis, which was larger than the mass gain caused by the addition of ozone molecules.[19] Lee and Chan[19] recently reported that about 5% of total particle mass evaporated for a completely reacted oleic acid particle.

Another possible reason for the observed particle mass gain is that direct ozonolysis of linoleic acid and linolenic acid only generate volatile species in low yields. This postulation is supported by the observed increase in the particle mass of linoleic acid and linolenic acid by about 5% and 10%, respectively, after 2 h of exposure in the high ozone concentration experiments. Although the details of reaction mechanisms cannot be verified in this study, it is possible that the polyunsaturated fatty acids and existing intermediate products provide significant amounts of active sites to react with Criegee intermediates. Since Criegee intermediates can also undergo isomerization to form short chain (<C9) carboxylic acids and some intermediate products are volatile or semi-volatile, the rapid reactions of Criegee intermediates with the polyunsaturated fatty acids and intermediate products would probably produce less volatile organics that would escape to the gas phase.

3.5. Changes in Hygroscopicity. The hygroscopicity of pure and ozone-processed linoleic acid and linolenic acid particles was measured using the EDB in the low ozone concentration experiments. Figure 11 shows the mass ratios (particle mass at a specific RH to particle mass at RH < 5%) of the linoleic acid and linolenic acid particles as a function of RH. The unreacted fatty acid particles are hydrophobic in nature and their mass ratios at RH ≈ 85% only increased by approximately 0.5−1%, which is within experimental uncertainty. After ozone exposure, the mass ratios of the ozone-processed linoleic acid and linolenic acid particles at RH ≈ 85% increased by about 2−3% and 3−4%, respectively. Although the change in hygroscopic growth was small, our measurements clearly show that the oxidation

Heterogeneous Reactions of Linoleic Acid

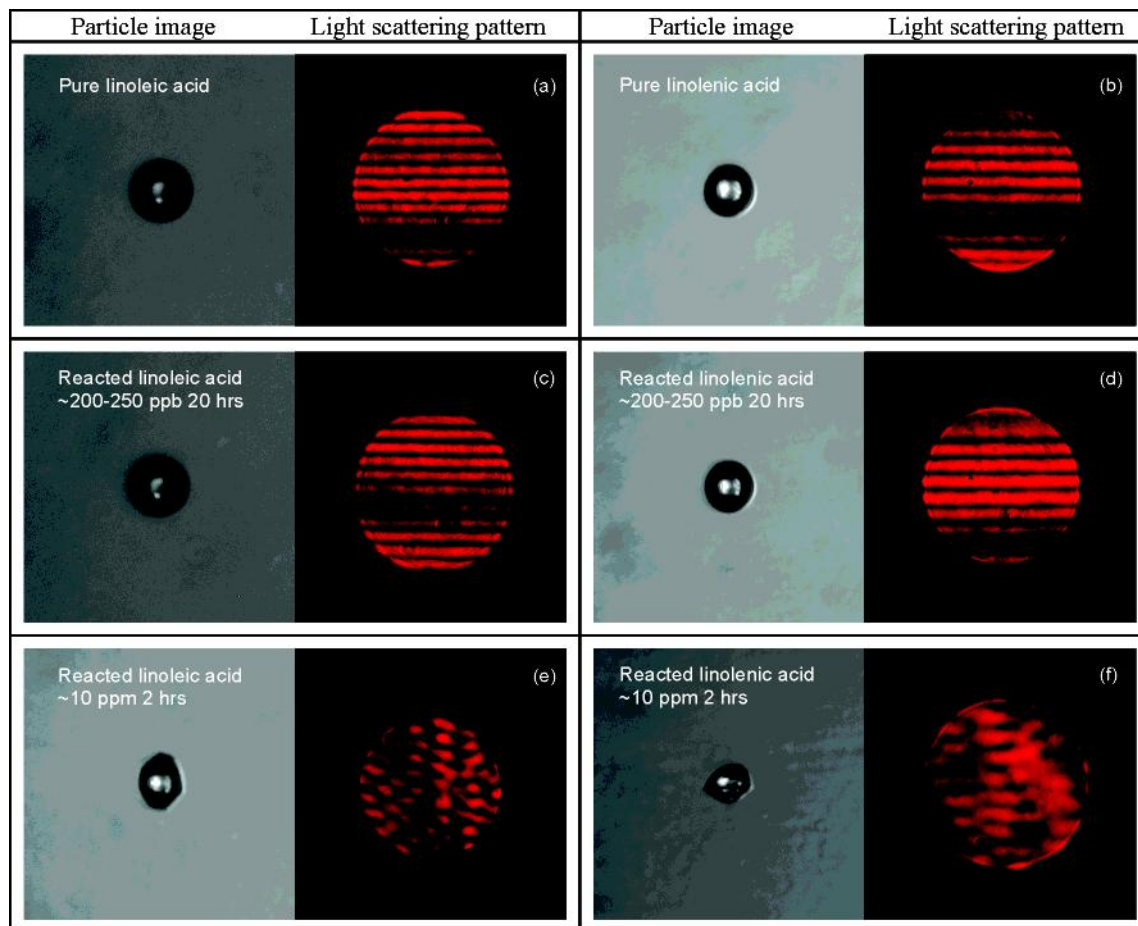*J. Phys. Chem. A, Vol. 111, No. 28, 2007* **6293**

Figure 12. Particle images and laser-illuminated light scattering patterns of the pure and ozone-processed linoleic acid (left-hand side) and linolenic acid particles (right-hand side).

products that remained in the particles are more hygroscopic than are their hydrophobic parent molecules, thus probably affecting the CCN activity of the particles. In addition, according to our hygroscopic measurements and visual observations using a microscope, both pure and ozone-processed linoleic acid and linolenic acid particles were in the liquid state, and no phase transition was observed.

3.6. Changes in the Particle Morphologies and Light Scattering Patterns. Particle images and laser-illuminated light scattering patterns were captured for pure and ozone-processed linoleic acid and linolenic acid particles. According to Figure 12a−d, the particles remained in spherical shapes before and after the reaction if the ozone concentration used was about 200−250 ppb. In addition, it is clearly observed that the laser-illuminated light scattering patterns, as presented in Figure 12a−d, of the pure and ozone-processed particles consisted of a few sharp horizontal lines, which supports that the particles had spherical shapes and were completely in liquid phase. In contrast, at very high ozone concentrations (∼10 ppm), the morphology and light-scattering patterns were appreciably modified as shown in Figure 12e−f. The particle shape changed from spherical to highly irregular under high ozone concentrations. The laser-illuminated light scattering patterns of the ozone-processed particles became irregular, which is evidence of the irregular particle shape or/and the formation of solid materials.

Our optical measurements show that there are some solid materials coated on the surfaces of the particles that make the particle shapes irregular when the fatty acid particles are exposed to extremely high ozone concentrations. It is particularly important to note that the solid coated particles absorbed a small

amount of water but the irregular particle shape and laser-illuminated light scattering pattern still could be observed when the RH inside the EDB was increased to 85−90% for about 3 h. This observation suggests that part of the solid materials coated on the surface of the ozone-processed particles may have relatively high deliquescence relative humidity (DRH) and possibly form a transport barrier for water uptake.[48] This finding may be useful to explain the results of CCN activity measurements obtained by Broekhuizen and co-workers.[23] They reported that there was no CCN activity enhancement in linoleic acid particles even under high ozone exposures not typically observed in the atmosphere (ozone concentration ≈ 3×10^{13} to 1×10^{16} molecules/cm^3 ≈ 0.8 to 400 ppm). They attributed their observations to the formation of highly branched and complex polymeric products. According to our observations, it is possible that there were some solid materials that completely covered the surfaces of the linoleic acid particles after such high ozone exposures, consequently limiting their CCN activity. Furthermore, the solid coating may also reduce the reactive uptake ability of atmospheric oxidants of organic aerosols.[20]

4. Conclusion and Atmospheric Implications

In this study, an EDB with a single particle Raman spectroscopic system was utilized to investigate the heterogeneous reactions of linoleic acid and linolenic acid with ozone. Our Raman measurements provided evidence that ozone-induced autoxidation, in addition to direct ozonolysis, is a plausible pathway in the reactions between ozone and linoleic acid and linolenic acid particles. Furthermore, the significance of this

specific oxidation pathway seems to depend on the ozone concentrations used in the experiment. Our finding indicates that a low ozone concentration (∼200−250 ppb) with a longer exposure period (20 h) favors autoxidation pathways while an extremely high ozone concentration (∼10 ppm) may force most of the unsaturated fatty acids to react with ozone in a relatively short period of time. The two-step kinetic behavior of the C=C−C=C peak intensity observed in the low ozone concentration experiments indicates that autoxidation products had accumulated at the beginning, and then they were lost via ozonolysis.

Autoxidation pathway is potentially important in the heterogeneous chemistry of organic aerosols because the ambient ozone concentrations are sufficiently high to initiate the autoxidation process as shown in this study. However, it is also possible that gas phase free radicals, such as OH and NO_3 radicals,[49,50] and particle phase organic/inorganic radicals produced via other heterogeneous processes can initiate autoxidation as well as other oxidative pathways, depending on their concentrations. The chemistry of the propagation step reported here is based on the reactions of pure polyunsaturated fatty acid particles. Linoleic acid and linolenic acid are important propagators of the autoxidation process as shown in Figures 4 and 5. For mixed atmospheric aerosol containing small amounts of alkenes, the peroxy radicals (ROO• in Figures 4 and 5) probably combine with each other, other free radicals or antioxidants (if any) to produce non-propagating species, consequently terminating the chain reactions. Nevertheless, autoxidation in atmospheric aerosols should not be ignored because free radicals are ubiquitous in ambient air as initiating species. To the best of our knowledge, this is the first time in the literature that the autoxidation pathway has been reported in the chemistry of atmospheric heterogeneous reactions. The significance of this specific oxidative process in atmospheric chemistry needs to be further explored.

Direct particle mass measurements using EDB show that the heterogeneous oxidation of organic aerosols can either increase or decrease the particle mass yields to different extents depending on the molecular structures of the chemical species and reaction pathways. In the low ozone concentration experiment, we found that the particle mass of oleic acid decreased by about 3−4% throughout the ozone exposure period, indicating the loss of volatile organic species through evaporation. In contrast, the mass of the ozone-processed linoleic acid and linolenic acid particles increased by about 2−3% and 10−13%, respectively. Although we did not measure particle size changes during the ozone exposure period, Broekhuizen et al.[23] reported that the particle size of ozone-processed oleic acid and linoleic acid were smaller than the original particles. In the case of linoleic acid, the particle density is, therefore, likely to be enhanced. This example illustrates that heterogeneous reactions are potentially important in modifying the particle density and subsequently the aerodynamic properties and the deposition characteristics of atmospheric organic aerosols.

Our hygroscopic measurements clearly show that the reaction products that remained in the particles are more hygroscopic than are their hydrophobic parent molecules. This is in accordance with our Raman results that the reaction products formed inside the particles are more oxygenated than pure unsaturated fatty acids. This finding implies that heterogeneous aging processes may have significant impacts on affecting the hygroscopicity and ultimately some physical properties (e.g., particle size, light scattering property, etc.) of atmospheric organic aerosols. Furthermore, both pure and ozone-processed

linoleic acid and linolenic acid particles were in the liquid state and no phase transition was observed in the low ozone exposure experiments. In contrast, there were some solid materials coated on the surfaces of the particles, make the particle irregular in shape when the fatty acid particles were exposed to extremely high ozone concentrations. The formation of such a coating affects the hygroscopic growth of the aged particles and likely their CCN activities.

Supporting Information Available: Figure S1, Raman spectra of oleic acid particles and reaction mixtures, and Figure S2, reaction pathways of the ozonolysis of oleic acid and possible reaction pathways involving stabilized Criegee intermediates. This material is available free of charge via the Internet at http://pubs.acs.org.

References and Notes

(1) Seinfeld, J. H.; Pandis, S. N. *Atmospheric Chemistry and Physics: from Air Pollution to Climate Change*, 2nd ed.; John Wiley & Sons: New York, 2006.

(2) Intergovernmental Panel on Climate Change (IPCC), *Climate Change: The Scientific Basis*; Cambridge University Press: Canbridge, U.K., 2001.

(3) Kanakidou, M.; Seinfeld, J. H.; Pandis, S. N.; Barnes, I.; Dentener, F. J.; Facchini, M. C.; Van Dingenen, R.; Ervens, B.; Nenes, A.; Nielsen, C. J.; Swietlicki, E.; Putaud, J. P.; Balkanski, Y.; Fuzzi, S.; Horth, J.; Moortgat, G. K.; Winterhalter, R.; Myhre, C. E. L.; Tsigaridis, K.; Vignati, E.; Stephanou, E. G.; Wilson, J. *Atmos. Chem. Phys.* **2005**, *5*, 1053.

(4) Saxena, P.; Hildemann, L. M.; McMurry, P. H.; Seinfeld, J. H. *J. Geophys. Res.* **1995**, *100*, 18755.

(5) Cruz, C. N.; Pandis, S. N. *Environ. Sci. Technol.* **2000**, *34*, 4313.

(6) Choi, M. Y.; Chan, C. K. *Environ. Sci. Technol.* **2002**, *36*, 2422.

(7) Cruz, C. N.; Pandis, S. N. *J. Geophys. Res.* **1998**, *103*, 13111.

(8) Abbatt, J. P. D.; Broekhuizen, K.; Kumal, P. P. *Atmos. Environ.* **2005**, *39*, 4767.

(9) Jang, M.; Czoschke, N. M.; Lee, S.; Kamens, R. M. *Science* **2002**, *298*, 814.

(10) Rudich, Y. *Chem. Rev.* **2003**, *103*, 5097.

(11) Kalberer, M.; Paulsen, D.; Sax, M.; Steinbacher, M.; Dommen, J.; Prevot, A. S. H.; Fisseha, R.; Weingartner, E.; Frankevich, V.; Zenobi, R.; Baltensperger, U. *Science* **2004**, *303*, 1659.

(12) Moise, T.; Rudich, Y. *J. Phys. Chem. A* **2002**, *106*, 6469.

(13) Smith, G. D.; Woods, E.; DeForest, C. L.; Baer, T.; Miller, R. E. *J. Phys. Chem. A* **2002**, *106*, 8085.

(14) Hearn, J. D.; Smith, G. D. *J. Phys. Chem. A* **2004**, *108*, 10019.

(15) Thornberry, T.; Abbatt, J. P. D. *Phys. Chem. Chem. Phys.* **2004**, *6*, 84.

(16) Hung, H. M.; Katrib, Y.; Martin, S. T. *J. Phys. Chem. A* **2005**, *109*, 4517.

(17) Zahardis, J.; LaFranchi, B. W.; Petrucci, G. A. *J. Geophys. Res.* **2005**, 110, D08307, doi:10.1029/2004JD005336.

(18) Ziemann, P. J. *Faraday Discuss.* **2005**, *130*, 469.

(19) Lee, A. K. Y.; Chan, C. K. *Atmos. Environ.* **2007**, *41*, 4611.

(20) Zahardis, J.; Petrucci, G. A. *Atmos. Chem. Phys.* **2007**, *7*, 1237.

(21) Zahardis, J.; LaFranchi, B. W.; Petrucci, G. A. *Atmos. Environ.* **2006**, *40*, 1661.

(22) Asad, A.; Mmereki, B. T.; Donaldson, D. J. *Atmos. Chem. Phys.* **2004**, *4*, 2083.

(23) Broekhuizen, K. E.; Thornberry, T.; Kumar, P. P.; Abbatt, J. P. D. *J. Geophys. Res.* **2004**, 109, D24206, doi:10.1029/2004JD005298.

(24) Rogge, W. F.; Hildemann, L. M.; Mazurek, M. A.; Cass, G. R.; Simoneit, B. R. T. *Environ. Sci. Technol.* **1993**, *27*, 2700.

(25) Schauer, J. J.; Kleeman, M. J.; Cass, G. R.; Simoneit, B. R. T. *Environ. Sci. Technol.* **1999**, *33*, 1566.

(26) Muik, B.; Lendl, B.; Molina-Díaz, A.; Ayora-Cañada, M. J. *Chem. Phys. Lipids* **2005**, *134*, 173.

(27) Pryor, W. A.; Stanley, J. P.; Blair, E.; Cullen, G. B. *Arch. Environ. Health* **1976**, *31*, 201.

(28) Pryor, W. A. *Free Radic. Biol. Med.* **1994**, *17*, 451.

(29) Davis, E. J. *Aerosol Sci. Technol.* **1997**, *26* (3), 212.

(30) Chan, C. K.; Flagan, R. C.; Seinfeld, J. H. *Atmos. Environ.* **1992**, *26*, 1661.

Heterogeneous Reactions of Linoleic Acid

J. Phys. Chem. A, Vol. 111, No. 28, 2007 **6295**

(31) Ha, Z.; Chan, C. K. *Aerosol Sci. Technol.* **1999**, *31*, 154.

(32) Zhang, Y. H.; Chan, C. K. *J. Phys. Chem. A* **2000**, *104*, 9191.

(33) Braun, C.; Krieger, U. *Opt. Expr.* **2001**, *8*, 314.

(34) Parsons, M. T.; Riffell, J. L.; Bertram, A. K. *J. Phys. Chem. A* **2006**, *110*, 8108.

(35) Olsen, A. P.; Flagan, R. C.; Kornfield, J. A. *Rev. Sci. Instrum.* **2006**, *77*, 073901.

(36) Bailey, P. S. *Ozonation In Organic Chemistry. Volume 1. Olefinic compounds*; Academic Press: New York, 1978.

(37) Rebrovic, L. *J. Am. Oil Chem. Soc.* **1992**, *69*, 159.

(38) Lin-Vien, D.; Colthup, N. B.; Fateley, W. G.; Grasselli, J. G. *The handbook of infrared and Raman characteristic frequencies of organic molecules*; Academic Press Inc.: San Diego, CA, 1991.

(39) Socrates, G. *Infrared and Raman Characteristic Group Frequencies: Tables and Charts*, 3rd ed.; John Wiley & Sons: Chichester, U.K., 2001.

(40) Kochhar, S. P. In *Deterioration of edible oils, fats and foodstuffs*; Chapter 2 of *Atmospheric oxidation and antioxidants*; Scott, G., Ed.; Elsevier Science Publishers, B. V: Amsterdam, Netherlands, 1993; Vol. 2.

(41) Porter, N. A.; Caldwell, S. E.; Mills, K. A. *Lipids* **1995**, *30*, 277.

(42) Niki, E.; Yoshida, Y.; Saito, Y.; Noguchi, N. *Biochem. Biophys. Res. Commun.* **2005**, *338*, 668.

(43) Gunstone, F. D. *J. Am. Oil. Chem. Soc.* **1984**, *61*, 441.

(44) Frankel, E. N. *J. Am. Oil. Chem. Soc.* **1984**, *61*, 1908.

(45) Frankel, E. N. *J. Sci. Food Agric.* **1991**, *54*, 495.

(46) Tachikawa, H.; Polaâsïek, M.; Huang, J. Q.; Leszczynski, J.; Salahudeen, A. K.; Kwiatkowski, J. S. *Appl. Spectrosc.* **1998**, *52*, 1479.

(47) Katrib, Y.; Martin, S. T.; Hung, H. M.; Rudich, Y.; Zhang, H.; Slowik, J. G.; Davidovits, P.; Jayne, J. T.; Worsnop, D. R. *J. Phys. Chem. A* **2004**, *108*, 6686.

(48) Chan, M. N.; Chan, C, K. *Atmos. Environ.* **2007**, *41*, 4423.

(49) Bertram, A. K.; Ivanov, A. V.; Hunter, M.; Molina, L. T.; Molina, M. J. *J. Phys. Chem. A*, **2001**, *105*, 9415.

(50) Moise, T.; Talukdar, R. K.; Frost, G. J.; Fox, R. W.; Rudich, Y. *J. Geophys. Res.* **2002**, *107*, D2, 4014.